PHYSICAL REVIEW B, VOLUME 63, 041401(R)

Intensities of the Raman-active modes in single and multiwall nanotubes

S. Reich and C. Thomsen
Institut für Festkörperphysik, Technische Universität Berlin, Hardenbergstrasse 36, 10623 Berlin, Germany

G. S. Duesberg and S. Roth
Max-Planck-Institut für Festkörperforschung, Heisenbergstrasse 1, 70569 Stuttgart, Germany

(Received 24 August 2000; published 9 January 2001)

We investigated the phonon symmetries in the Raman spectra of single and multiwall nanotubes. By using linearly and circularly polarized light we measured the Raman tensor invariants on unoriented carbon nanotubes. The ratio between the antisymmetric and the isotropic invariant shows that Raman scattering in semiconducting single wall tubes is mainly due to fully symmetric $A_{1(g)}$ phonons with a strongly uniaxial Raman tensor. With the help of recent experiments on aligned nanotubes we calculate the relative intensities for the high-energy modes of different symmetry. Compared to single wall tubes the intensity of the $E_{1(g)}$ and $E_{2(g)}$ symmetry phonons in multiwall tubes is 1.5 times stronger. The antisymmetric component of the resonant Raman process was found to be zero in all measurements.

DOI: 10.1103/PhysRevB.63.041401 PACS number(s): 78.30.Na, 63.20.Kr, 63.22.+m

The vibrational properties of carbon nanotubes are still a puzzling part of this extensively studied system. The modes which are observable by Raman spectroscopy fall into two different energy regions, the low-energy modes around $200\,\mathrm{cm}^{-1}$ and the high-energy modes between 1500 and $1600\,\mathrm{cm}^{-1}$. The low-energy Raman signal originates from a breathinglike vibration of the tube; its energy is determined by both inter- and intramolecular force constants.[1–3] For a single tube this mode has a purely radial A_{1g} (armchair and zig-zag tubes) or A_1 (chiral tubes) eigenvector. The frequency of the Raman peak depends on the diameter of the nanotubes and on the excitation energy. As was shown by Milnera *et al.*[3] the radial breathing mode is resonant throughout the visible; the different frequencies stem from nanotubes of different size. Incoming and outgoing resonances also determine the shape of the high-energy Raman spectrum.[4–7] The spectrum of semiconducting tubes, excited, e.g., with a blue laser line, is dominated by two broad peaks around 1592 and 1565 cm^{-1}, whereas the metallic nanotube spectra (red excitation) extends down to 1540 cm^{-1}.

In contrast to the radial breathing mode, the assignment of the Raman peaks to phonon symmetries and eigenvectors is still an open question for the high-energy modes. Phonons in this energy range have eigenvectors similar to the graphite optical E_{2g} mode and a displacement parallel to the nanotube circumference or to the z axis. If the envelope function is without nodes along the circumference the phonon belongs to the A_1 or A_{1g} representation; $E_{1(g)}$ modes have two nodes around the circumference, $E_{2(g)}$ modes four. Recently, Raman measurements on aligned single and multiwall nanotubes were published.[8–10] It was found that Raman scattering in (z,z) configuration is strongest in both types of tubes. On very small semiconducting single wall tubes (diameter $d=5$ Å) two peaks with A_1 and E_2 components were observed and one with E_1 symmetry.[8,11] Distinct peaks were not detected in the multiwall species, but the overall Raman intensity was different in the four scattering geometries.[9] The Raman experiments published so far were carried out in backscattering configuration perpendicular to the nanotubes axis. In this configuration, it is impossible to distinguish the $A_1(x,x)$ component from E_2 contributions in the Raman spectra.

The symmetries of the scattering phonons can also be studied by measuring the Raman tensor invariants on unoriented samples. In this paper we report the tensor invariants of single and multiwall nanotubes, which we obtained by linearly and circularly polarized Raman measurements. We find that in semiconducting single wall nanotubes both the high and low-energy vibrations are dominated by totally symmetric scattering with a strongly uniaxial Raman tensor. The spectra of multiwall nanotubes show a higher value of the anisotropic tensor invariant, which is indicative for traceless E symmetry. We found the antisymmetric invariant to be zero in our measurements. With the help of the experiments on aligned nanotubes we are able to determine the elements of the A_1, E_1, and E_2 Raman tensors normalized to the $A_1(z,z)$ component and their relative intensities in the Raman spectra.

The Raman tensor is usually expressed as a second rank Cartesian tensor and decomposed into the irreducible representations of the molecular or crystal point group.[12] In a bulk crystal, the tensor elements α_{ij} $(i,j=x,y,z)$ can be determined in the proper scattering configurations. If, however, the sample consists of unoriented scatterers the intensities in a Raman experiment are averaged over all orientations. At first sight this seems to frustrate the use of polarized light to determine the phonon symmetry, but it is still possible to find the tensor invariants and to distinguish between the symmetries belonging to different irreducible tensors.[13,14] The traditional invariants used in Raman spectroscopy are the isotropic part[13]

$$\overline{\alpha^2}=\frac{1}{9}(\alpha_{xx}+\alpha_{yy}+\alpha_{zz})^2, \tag{1}$$

the symmetric anisotropy

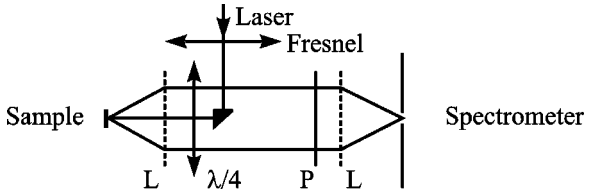

FIG. 1. Schematic picture of the setup. The light coming from the laser is vertically polarized.

$$\gamma_s^2=\frac{1}{2}[(\alpha_{xx}-\alpha_{yy})^2+(\alpha_{yy}-\alpha_{zz})^2+(\alpha_{zz}-\alpha_{xx})^2]$$

$$+\frac{3}{4}[(\alpha_{xy}+\alpha_{yx})^2+(\alpha_{xz}+\alpha_{zx})^2+(\alpha_{yz}+\alpha_{zy})^2], \quad (2)$$

and the antisymmetric anisotropy

$$\gamma_{as}^2=\frac{3}{4}[(\alpha_{xy}-\alpha_{yx})^2+(\alpha_{xz}-\alpha_{zx})^2+(\alpha_{yz}-\alpha_{zy})^2]. \quad (3)$$

In nonresonant Raman scattering γ_{as}^2 is zero, but antisymmetric scattering might evolve under resonance. Representations giving rise to antisymmetric scattering are $E_{1(g)}$ and the totally antisymmetric ($\alpha_{ij}=-\alpha_{ji}$) $A_{2(g)}$ representation. All symmetries except the totally symmetric $A_{1(g)}$ have $\overline{\alpha^2}=0$. For $A_{1(g)}$ phonons $\overline{\alpha^2}\neq 0$ and $\gamma_s^2\neq 0$ in the D_q and D_{2nh} point groups of chiral and achiral nanotubes.[15,14,12]

The measurements of the Raman tensor invariants on unoriented samples is performed using linearly and circularly polarized light. In backscattering geometry, the invariants are given by[13,16]

$$45\overline{\alpha^2}=I_{\parallel}-\frac{2}{3}I_{\circlearrowleft\circlearrowleft},$$

$$6\gamma_s^2=I_{\circlearrowleft\circlearrowleft},$$

$$5\gamma_{as}^2=I_{\perp}-\frac{1}{2}I_{\circlearrowleft\circlearrowleft}, \quad (4)$$

where $I_{\parallel}$ is the intensity with the incoming and scattered light linearly parallel polarized, $I_{\perp}$ in crossed linear polarization, and $I_{\circlearrowleft\circlearrowleft}$ is the intensity in corotating circular polarization. The experimental error can be checked by $|(I_{\parallel}+I_{\perp})-(I_{\circlearrowleft\circlearrowleft}+I_{\circlearrowleft\circlearrowright})|=\Delta I$, where $I_{\circlearrowleft\circlearrowright}$ denotes the intensity in contrarotating circular polarization.

The experimental setup for measuring the intensities in parallel, crossed, corotating, and contrarotating polarization without change in the illumination is depicted in Fig. 1.[13] The incoming linearly polarized laser light passes through a Fresnel romb and a λ/4 zero-order wave plate after which it is focused (L) onto the sample. The scattered light travels backwards through the λ/4 wave plate, is analyzed with a polarization filter (P), and focused (L) onto the entrance slits of a triple-grating spectrometer equipped with a CCD detector. We checked the positions of the polarizing elements by the Raleigh scattered light and by the known tensor invariants of the CCl_4 Raman peaks. For excitation we used the 488 nm line of an Ar/Kr laser. The single wall sample was a free standing film of bucky paper prepared from Tubes@Rice nanotubes (mean diameter 1.2 nm). The multiwall nanotubes were grown by the arc-discharge method.

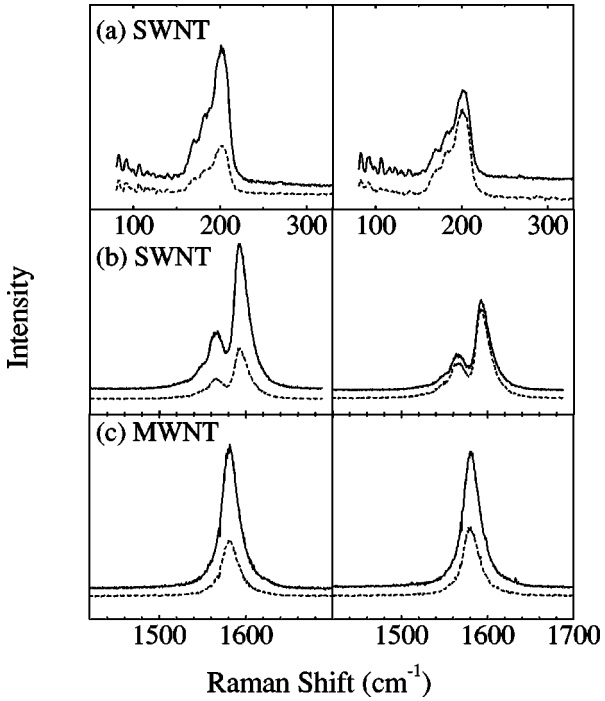

FIG. 2. Raman spectra of single and multiwall nanotubes in linear (left) and circular (right) polarizations. The full lines are the spectra in parallel (left) and corotating (right) polarization; the dashed lines in crossed and contrarotating polarization. The spectra are shifted vertically; the scales in the corresponding right and left pictures are the same.

In Fig. 2 we show the Raman spectra of the low- (a) and high-energy (b) modes of single wall nanotubes and in Fig. 2(c) the high-energy modes in multiwall tubes. On the left and right side are the spectra measured in linear and circular polarization, respectively. The spectral shape is independent of the polarization; only the overall intensity of the spectra changes. This demonstrates that the Raman peaks are not due to modes of distinct, different symmetry; instead a superposition of mainly A_1 and weaker E contributions is observed. The tensor invariants obtained from the spectra and Eq. 4 are given in Table I in arbitrary units together with ΔI and the ratio of $\gamma_s^2/\overline{\alpha^2}$, which is indicative of the phonon symmetry. For comparison we also list the invariants of the graphite E_{2g} optical mode. According to Eqs. (1)–(3) the only nonzero invariant for E_{2g} symmetry is γ_s^2; indeed $45\overline{\alpha^2}$ and $5\gamma_{as}^2$ are within the experimental error.[13] The large value of $\gamma_s^2/\overline{\alpha^2}=170$ confirms the traceless symmetric Raman tensor of the scattering phonon. In carbon nanotubes, the phonon symmetries are less obvious from the experiments. Clearly, the antisymmetric invariant γ_{as}^2 is zero in all measurements and therefore (i) $A_{2(g)}$ do not contribute to the spectra and (ii) the two nonvanishing Raman matrix elements of the $E_{1(g)}$ modes are equal. The rather small ratios $\gamma_s^2/\overline{\alpha^2}$ point to a

TABLE I. Tensor invariants (arb. units) of the Raman modes in semiconducting single wall and multiwall tubes and graphite. Quantities comparable to the experimental error ΔI can be considered zero.

Frequency (cm^{-1})		$45\overline{\alpha^2}$	$6\gamma_s^2$	$5\gamma_{as}^2$	ΔI	$\gamma_s^2/\overline{\alpha^2}$
SWNT	1594	204	252	3	50	9.3
	1565	64	80	1.5	20	9.3
	1554	20	26	1.4	2	9.7
	202	19	24	-0.3	3	9.6
	183	7.8	9.6	0.04	0.7	9.2
	167	3.6	5.0	0.1	0.8	10.3
MWNT	1581	2.5	5.8	0.8	0.5	17.2
graphite	1582 (E_{2g})	0.72	16.3	0.4	1	170

strong fully symmetric component, since these are the only modes with a finite isotropic part $\overline{\alpha^2}$ [see Eq. (1)].

In general, the ratio $\gamma_s^2/\overline{\alpha^2}$ stemming from the superposition of an A_1 ($\alpha_{xx}=\alpha_{yy}=a,\alpha_{zz}=b$), an E_1 ($\alpha_{xz}=\alpha_{zx}=\alpha_{yz}=\alpha_{zy}=c$), and an E_2 ($\alpha_{xx}=-\alpha_{yy}=\alpha_{xy}=\alpha_{yx}=f$) Raman tensor is given by

$$\frac{\gamma_s^2}{\overline{\alpha^2}}=\frac{9[(a-b)^2+6(c^2+f^2)]}{(2a+b)^2}. \tag{5}$$

For the radial breathing mode we can safely assume $c=f=0$; here and in the following we normalize to $b=1$. The two possible values of a which yield the measured ratio between the anisotropic and isotropic part are $a\approx 0$ and -2. Whereas the first result implies a small matrix element in (xy) compared to z polarization, the second results predicts the (xy) intensity to be four times stronger. The resonant Raman matrix element is determined by the optical absorption probability and the electron-phonon coupling. Although the deformation potential interaction should be stronger in (xy) for the eigenvector under consideration, which was confirmed by nonresonant calculations of the Raman intensities,[17] in the resonant situation typical for carbon nanotubes the optical transition probability dominates the intensities.[3,12] The optical absorption for light polarized perpendicular to the z axis seems to be vanishingly small in carbon nanotubes.[6,18] Thus the first solution $-0.02\leqslant a\leqslant 0$ is the correct one and scattering by the radial-breathing mode is dominated by the intensity in (z,z) polarization. This is also consistent with the measurements on small single wall[8] and metallic nanotubes.[10]

For the high-energy modes in single and multiwall nanotubes we expect contributions by the totally symmetric as well as the E symmetry modes, i.e., there are three unknown variables in Eq. (5). To obtain the Raman matrix elements a, c, and f and the relative scattering intensities we use the measurements on aligned nanotubes.[8,9] After integrating over the xy plane the intensities in the Raman configurations are $I(z,z)=b^2=1$, $I(xy,xy)=a^2+f^2$, and $I(xy,z)=I(z,xy)=c^2$. The experimentally obtained values are summarized in Table II. Note the small xy intensities in single wall nanotubes as compared to (z,z) scattering.[8,10]

TABLE II. Relative intensities in parallel and crossed polarization normalized to the (z,z) intensity. For multiwall nanotubes different values for (xy,z) and (z,xy) geometry and two values for $I(xy,xy)$ were reported (compare Figs. 1 and 3 in Ref. 9). The ratio in the last row was calculated from the mean value. The intensities in single wall nanotubes are weighted by the width of the Raman peaks in Ref. 8.

	MWNT (Ref. 9)	SWNT (Ref. 8)		
Frequency (cm^{-1})	1584	1615	1599	1585
$I(xy,xy)$	0.29, 0.5	0.1	0.02	0.05
$I(xy,z)$	0.19, 0.39	0.01	0.16	0.01
$I(xy,z)/I(xy,xy)$	0.75		1	

In Fig. 3 we show the decomposition of the scattering intensity into the (xx) component of the A_1 (a^2, full lines), the E_1 (c^2, dashed lines), and the E_2 (f^2, dotted lines) modes in single and multiwall nanotubes as a function of the (xy,xy) scattering intensity. Figure 3(a) refers to multiwall nanotubes, i.e., $\gamma_s^2/\overline{\alpha^2}=17$ and $I(xy,z)/I(z,z)=0.75$ (compare Tables I and II). The dashed vertical line at 0.4 denotes the experimental results of Rao *et al.*[9] Most of the intensity in (xy,xy) polarization in multiwall nanotubes originates from scattering by E_2 symmetry phonons, which have a relative intensity of 0.33 as compared to the A_1 contribution of 0.07. The E_1 intensity (0.3) is fully determined by the value measured in crossed polarization. The larger E_2 contribution compared to $A_1(xx)$ and E_1 is reasonable in multiwall tubes; in the limit of d approaching infinity all intensity is transferred to the E_{2g} graphite mode. This is nicely seen in Fig. 3(b) where we plotted the relative intensities with the same ratio between the intensities in parallel and crossed polarization but $\gamma_s^2/\overline{\alpha^2}=9$ as measured on single wall nanotubes. The E_2 contribution drops down to 0.22 whereas the $A_1(xx)$

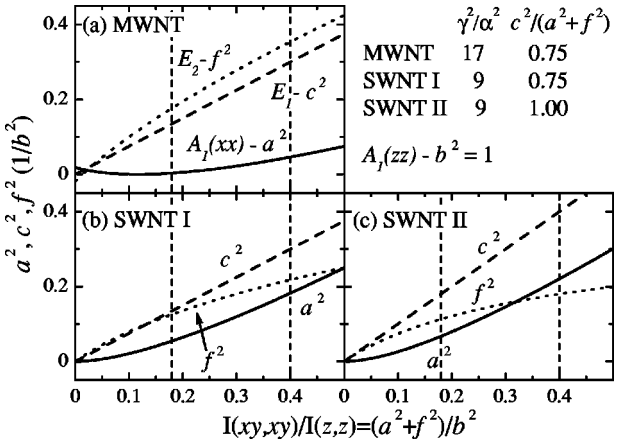

FIG. 3. Raman matrix elements as a function of the intensity in (xy,xy) polarization. (a) calculated with the tensor invariants of multiwall tubes $\gamma_s^2/\overline{\alpha^2}=17$ and $I(xy,z)/I(xy,xy)=c^2/(a^2+f^2)=0.75$ as measured by Rao *et al.* (Ref. 9); (b) same as (a) but with the invariants of single wall tubes (see upper right part of the figure); (c) same as (a) for single wall tubes and the results of Sun *et al.* (Ref. 8).

intensity is raised to 0.18. Figure 3(c) refers to the relative intensities obtained by Sun *et al.*[8] At the measured $I(xy,xy)=0.18$ the $A_1(xx)$ component is again below 0.1 as in multiwall nanotubes. The E_1 and E_2 contributions are around 0.2 and 0.1, respectively. The smaller E components can be understood by considering the enhancement of the Raman intensity by resonant transitions: The strength of an incoming resonance depends on the energy separation ΔE to the next real electronic band having the same symmetry as the scattered intermediate state, similarly for an outgoing resonance. Whereas the A_1 modes couple bands of the same symmetry, scattering by E modes always changes the symmetry of the electronic wave function. Since the separation between the electronic singularities scales as $1/d$ the resonances of the E phonons are weaker for smaller nanotubes. Typical single wall nanotubes have diameters between 1 and 1.5 nm. Consequently, scattering by E_1 and E_2 modes is a little more pronounced than in the $d=5$ Å tubes studied in Ref. 8, but still the intensities are small compared to the A_1 contribution in (z,z) configuration. A surprising result is the very small $a=\alpha_{xx}=\alpha_{yy}$ Raman matrix element. The scattering intensity of the fully symmetric mode in (xy,xy) configuration is even weaker than the intensity due to E symmetry modes. Because the transition probability for optical absorption and emission has a similar influence on the E and A_1 modes, the low A_1 intensity suggests small xx and yy electron-phonon matrix elements.

In conclusion, we measured the tensor invariants of the Raman active modes in semiconducting single wall and multiwall nanotubes. The high-frequency Raman modes originate from a superposition of A_1, E_1, and E_2 phonon symmetries; most of the intensity is due to (z,z) polarized scattering by A_1 phonons of different frequency. In contrast, the xx and yy elements of the A_1 Raman tensor are very small, yielding less than 5% of the overall intensity. In single wall nanotubes the second strongest contribution to the high-energy Raman spectra comes from scattering by E_1 modes. Their intensity is around 15% of the total scattering. The contribution by E_2 modes is a little lower around 10%. In multiwall nanotubes much of the scattering intensity is transferred to E_1 and E_2 phonons, which together now account for 40% of the total scattering. Consequently, the ratio between the anisotropic and the isotropic tensor invariant is larger in multiwall $\gamma_s^2/\overline{\alpha^2}=17$ than in single wall $\gamma_s^2/\overline{\alpha^2}=9$ nanotubes. The stronger E symmetry scattering is due to (i) relatively stronger resonances of the E modes in larger tubes compared to the A_1 resonances, because the energetic separation between the electronic bands is smaller and (ii) a stronger contribution by the E_2 symmetries for larger diameters since this is the allowed symmetry for graphite Raman modes.

Note added: A recently published polarized Raman study on aligned single wall nanotubes compares well with our results.[19] With the reported $I(xy,z)/I(xy,xy)=0.8$ and $I(xy,xy)/I(z,z)=0.25$ we obtain similar intensities as given above. Jorio *et al.*, however, based on nonresonant calculations concluded that E_2 modes do not contribute to the two most intense peaks.[19] The Raman tensors they proposed yield with Eq. (5) $\gamma_s^2/\overline{\alpha^2}\approx 3$ or ∞ depending on the sign of a and b. This demonstrates the additional benefit of our approach which yields the relative intensities without further theoretical assumptions.

[1] U. D. Venkateswaran, A. M. Rao, E. Richter, M. Menon, A. Rinzler, R. E. Smalley, and P. C. Eklund, Phys. Rev. B **59**, 10 928 (1999).

[2] C. Thomsen, S. Reich, A. R. Goñi, H. Jantoljak, P. Rafailov, I. Loa, K. Syassen, C. Journet, and P. Bernier, Phys. Status Solidi B **215**, 435 (1999).

[3] M. Milnera, J. Kürti, M. Hulman, and H. Kuzmany, Phys. Rev. Lett. **84**, 1324 (2000).

[4] A. Kasuya, *et al.*, Phys. Rev. B **57**, 4999 (1998).

[5] M. A. Pimenta, *et al.*, Phys. Rev. B **58**, R16 016 (1998).

[6] H. Kataura, Y. Kumazawa, Y. Maniwa, I. Umezu, S. Suzuki, Y. Ohtsuka, and Y. Achiba, Synth. Met. **103**, 2555 (1999).

[7] P. M. Rafailov, H. Jantoljak, and C. Thomsen, Phys. Rev. B **61**, 16 179 (2000).

[8] H. Sun, Z. Tang, J. Chen, and G. Li, Solid State Commun. **109**, 365 (1999).

[9] A. M. Rao, A. Jorio, M. A. Pimenta, M. S. S. Dantas, R. Saito, G. Dresselhaus, and M. S. Dresselhaus, Phys. Rev. Lett. **84**, 1820 (2000).

[10] G. S. Duesberg, I. Loa, M. Burghard, K. Syassen, and S. Roth, Phys. Rev. Lett **85**, 5436 (2000).

[11] The authors of Ref. 8 concluded a little different. However, they normalized the maximum peak intensity in each configuration to unity, which is not a valid procedure. When comparing directly, e.g., the intensities of the 1585 cm^{-1} peak in (z,z) and (xy,xy) configuration in Fig. 3 of Ref. 8 it becomes obvious that this peak is not of E_{2g} symmetry; it is stronger in (z,z) than in (xy,xy) configuration.

[12] M. Cardona, in *Light Scattering in Solids II*, edited by M. Cardona and G. Güntherodt (Springer, Berlin, 1982).

[13] J. Nestor and T. G. Spiro, J. Raman Spectrosc. **1**, 539 (1973).

[14] W. M. McClain, J. Chem. Phys. **55**, 2789 (1971).

[15] M. Damnjanović, I. Milošević, T. Vuković, and R. Sredanović, Phys. Rev. B **60**, 2728 (1999).

[16] S. Reich and C. Thomsen, Phys. Rev. Lett. **85**, 3544 (2000).

[17] R. Saito, T. Takeya, T. Kimura, G. Dresselhaus, and M. S. Dresselhaus, Phys. Rev. B **57**, 4145 (1998).

[18] H. Ajiki and T. Ando, Jpn. J. Appl. Phys., Suppl. **34-1**, 107 (1994).

[19] A. Jorio, *et al.* Phys. Rev. Lett. **85**, 2617 (2000).